Journal of Geosciences, Osaka City University
Vol. 46, Art. 13, p. 207-216, March, 2003

JERS-1 Interferometric SAR DEM Generation and Validation in Safaga Area, Red Sea Coast of Egypt

Alaa MASOUD[1], Venkatesh RAGHAVAN[2], MASUMOTO Shinji[1], and SHIONO Kiyoji[1]

[1]Department of Geosciences, Faculty of Science, Osaka City University, 3-3-138 Sugimoto, Sumiyoshi-ku, Osaka 558-8585, Japan. Corresponding author's e-mail address: alaa1999@sci.osaka-cu.ac.jp
[2]Media Center, Osaka City University, 3-3-138 Sugimoto, Sumiyoshi-ku, Osaka 558-8585, Japan.

Abstract

Digital elevation models (DEMs) and their products are widely used for numerous geoscientific applications. However, at the present time, good quality DEMs is lacking in several areas and efforts have to be made to generate such DEMs by various means. Spaceborn synthetic apertur radar interferometry (InSAR) has made possible accurate and rapid generation of DEMs. The potential gain from interferometry is significant, since accuracy measurements can be determined to within a resolution element of wavelength dimension. However, the quality and accuracy of DEM generated through InSAR needs to be carefully accessed before the data can be put to practical use. In this paper, an attempt has been made to generate large scale DEM for Safaga area on the Red Sea Coast of Egypt exploring the merits of the InSAR technique. Repeat-pass L-band JERS-1 SAR data acquired on 12 January 1994 and 10 June 1996 with a baseline length of 334.18 m are processed utilizing GAMMA SAR interferometry processing system. An interferometric DEM is generated at 28.5 m grid spacing and validated against a suite reference DEM tailored from 1:50,000 topographic map showing well agreement. However, there are several aspects in the data selection and processing scheme has to be optimized in terms of performance, accuracy and time to obtain the desired results. These aspects are highlighted and results are shown to demonstrate the expected accuracies using JERS-1 SAR data in DEM generation practices.

Key-words : SAR interferometry, DEM, Safaga Area, Red Sea Coast, Egypt.

1. Introduction

SAR interferometry (InSAR) is becoming a consolidated technique for accurate DEM production. The maturity of this technique, the high spatial resolution, good potential precision, the highly automated DEM generation capabilities, and the wide variability of SAR data, make the DEM generation attractive and affordable to an ever-wider user community. DEMs with good accuracy and large scale are not available for many areas in the world and InSAR is promising to overcome this lack of DEMs. InSAR was proposed by Graham in 1974 and applied for the first time at JPL (Jet Propulsion Laboratories) in 1986 using airborne data (Zebker and Goldstein, 1986). Today, a large number of research groups are working on DEM generation with InSAR data coming from different airborne and spaceborne systems. Repeat-pass InSAR technique depicts the pixel-by-pixel difference in the radar phases of a pair of single look complex (SLC) data sets acquired from displaced vantage points by a single sensor at dif-

ferent times. This phase difference (known as interferogram) corresponds to the difference in the round-trip path length of radar waves to ground targets and is a function of the distance between satellite passes (satellite baseline), terrain, and possibly surface changes. When surface changes are negligible, the interferograms basically represent surface topography. There is a number of excellent sources describe the theory and mathematics of the InSAR technique (Alaska SAR Facility, 1999; Massonet, 1997; Zebker and Villasenor, 1992).

While the InSAR basic technique is well studied and understood and the tool is available to prepare and process the data, there are several aspects in the data selection and processing scheme to be optimized in terms of performance, accuracy and time that in turn affect the quality of the derived products such as coherence maps, interferograms and the final height models. Such aspects need to be taken into account to achieve the accuracy and the quality desired for the interferometric products.

This paper describes the generation of 28.5 m spacing DEM for Safaga area on the Red Sea coast of Egypt (Fig. 1) utilizing L-band two-pass JERS-1 SAR data acquired on 12 January 1994 and 10 June 1996 utilizing GAMMA SAR interferometry processing system (Werner et al., 2000). DEM at 28.5 m resolution will be integrated with Landsat TM 5 imagery covering the study area for future environmental investigations. The basic approach for InSAR processing is briefly described, with special attention devoted to the aspects of the SAR data acquisition, processing chain, and post-processing relevant to DEM generation is highlighted. Validation of the geocoded InSAR height model is carried out using a suite reference DEM derived from topographic maps to explore the potential and limitations of the SAR technique. Results derived from such computational technique are presented and evaluated, and conclusions are drawn.

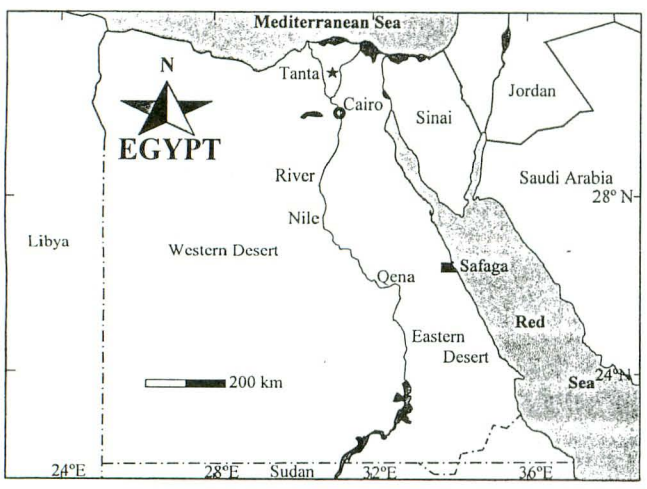

Fig. 1 Location map of the study area.

2. InSAR for DEM generation

2.1. SAR background

Repeat-pass InSAR technique estimates the difference (pixelwise) between the radar phases of a pair of SAR data sets acquired for the same terrain from slightly displaced points by a single sensor at different times. This phase difference pattern can be related to the surface topography when there no surface changes are countered. For repeat-pass imaging geometry, topography depends only on the phase information and the system parameters (baseline length, used wavelength etc.), not on the interferometric magnitude. Basic imaging geometry for repeat-pass JERS-1 SAR together with some orbit/radar specifications is shown in figure 2.

With reference to figure 2, the phase difference φ between the two radar signals received from the same surface element at the two antenna positions according to Li and Goldstein (1990) can be calculated as:

$$\varphi = 4\pi(\delta r)/\lambda = 4\pi(B_h \sin\theta - B_v \cos\theta)/\lambda \qquad (1)$$

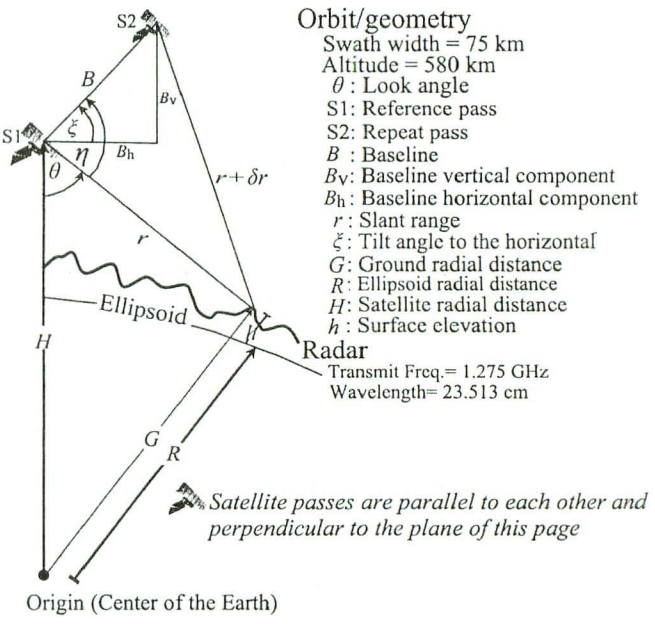

Fig. 2 JERS-1 SAR geometry with some orbit/radar specifications.

Where λ is the wavelength and δr is the range difference. Based on the range difference that in turn is based on SAR geometry of the side looking angle and the baseline components, the phase difference (interferometric phase) between two sensor positions and the target terrain point (pixelwise) can be generated. The resulted interferogram following coherence estimation and adaptive filtering shows the differences in phase, but only in terms of 2π. Phase unwrapping sums these 2π terms across the scene to calculate the total difference. The resulted unwrapped phase is almost linearly proportional to the topographic height.

For height map generation, unwrapped phase together with the precision refined baseline are then used to derive the topographic heights and true ground ranges. The height of each pixel above the reference ellipsoid can be simply given by:

$$h=\sqrt{H^2+r^2-2H\ r\cos\theta}-R \quad (2)$$

$$h=\sqrt{H^2+r^2-2H\ r(\sin\eta B_h/B-\cos\eta B_v/B)}-R \quad (3)$$

From the ellipsoid information together with the geoidal heights of the Mean Sea Level (MSL) through the study area, topographic elevations from the MSL can be determined for every pixel in the scene and the resulted height model can be georeferenced to the orthonormal map coordinates.

2.2. Data selection and InSAR processing

2.2.1. Data selection

Data selection is the first task required to obtain good quality interferometric products. Repeat pass SAR interferometry at L-band can be appraised for the generation of digital elevation models under certain conditions. The most important is that there is sufficient correlation to generate fringes over the area. Several factors contribute to the decorrelation including baseline decorrelation, thermal noise, changes in the Doppler centroid between the passes, surface slope, and temporal decorrelation of the surface (Zebker and Villasenor, 1992).

By far the most significant of these factors are the temporal and the baseline decorrelation. Temporal decorrelation is the change of the surface backscatter between the two passes. Baseline decorrelation is a direct result of a shift in the reflectivity spectrum caused by the change in incidence angle for the two passes. The baseline must be large enough to guarantee sufficient height sensitivity and not too short to achieve a good spatial resolution (Zebker and Villasenor, 1992; Massonnet, 1995). Based on minimal temporal decorelation and a suitable baseline length of 334.18 m, selection of JERS-1 data for the generation of the DEM is justified.

2.2.2. InSAR processing

DEM generation through spaceborne SAR interferometry is a complex undertaking that works best when coherence, phase unwrapping, and baseline (height sensitivity) constraints are all balanced optimally and satisfied. Many non-trivial steps are necessary to optimize the processing parameters to properly extract useful and accurate information from the raw data.

SAR processing was carried out on the JERS-1 raw data using the GAMMA SAR interferometry processing system comprising of a calibrated range/Doppler processor, interferogram calculation using applying spectral filtering, adaptive non-linear filtering of the interferogram, and phase unwrapping using a residue approach (Werner *et al.*, 2000).

Mainly three processing steps are enacted for DEM generation involving; Modular SAR processing (MSP), Interferometric SAR processing (ISP) and Geocoding. Flow chart showing the GAMMA SAR interferometry processing chain for the production of an interferometric DEM is shown in Fig. 3, and is briefly presented in order in the following basic points:

Modular SAR processing (MSP) to focus the two raw data into Single-Look Complex (SLC) SAR and Multi-look Intensity (MLI) images of the radar signals. Fig. 4a shows the master 12 January 1994 multi-look intensity (MLI) image.

Interferometric SAR processing (ISP) comprising:

(1) Precision coregistration and spectral band filtering for the two SLCs and resampling the slave image to be in register with the master image. Good coregistration at sub-pixel accuracy and spectral band filtering of the two single-look complex images increases the coherence estimates that in turn improve the quality of the final products.

(2) Interferogram generation by a simple pixel-wise complex multiply of the master image times the conjugate of the coregistered slave image. The interferogram (Fig. 4b), up to this point, records phase differences ($-\pi$ to π) that result from topography, which is the objective of this study and the flat earth phase, and is due to simple geometry of the satellites with respect to each other. Flat earth phase is then removed to flatten the interferogram, leaving only the component due to topography (Fig. 4c).

(3) Coherence is a measure of the temporal decorrelation between data acquisitions and is the key factor controlling the accuracy and the quality of the interfeometric products. Coherence is estimated by a

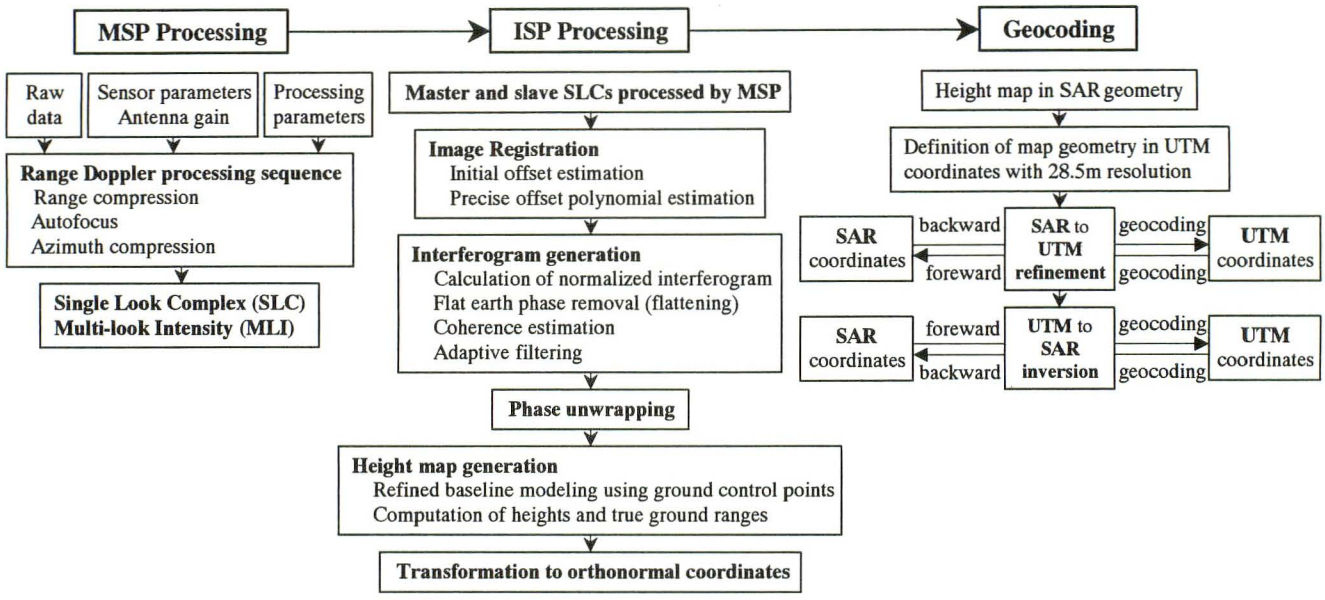

Fig. 3 Flow chart of SAR processing chain.

complex correlation between the master and coregistered slave images. The cross correlation operation is performed over a small local area surrounding each pixel in the interferogram. The area size should be suitable enough to get a good correlation estimate with good spatial resolution. Coherence ranges from 0 to 1. Fig. 4d shows the corresponding coherence image, in which color corresponds to interferometric coherence and brightness to backscatter intensity, yellow colors refer to high coherence and bright blue colors point to low coherence.

(4) Adaptive filtering for the flattened interferogram to reduce phase noise employing a narrower bandwidth in low coherence areas and a wider bandwidth in high coherence areas.

(5) Phase unwrapping consists of removing the cyclical ambiguity in the interferometric phase measurements (only moduli of 2π) by summing these 2π terms across the scene to calculate the total difference utilizing region-growing algorithm (Rosen *et al.*, 1994). Residue connection-based algorithm was applied to convert the interferometric phase to topographic phase. The algorithm attempts to connect phase discontinuities called residues in some manner that prevents phase unwrapping errors (Goldstein *et al.*, 1988). The resulted unwrapped interferometric phase with a color cycle of 0 to 2π is shown in Fig. 4e.

(6) Phase-to-height conversion from an unwrapped phase values to a height data with units of meters in pixel-wise scaling that requires accurate knowledge of the time varying baseline. A least squares fit for 40 ground control points well-distributed through the scene and shown on Fig. 4 a, extracted from 1:50,000 topographic maps covering Safaga area (Egyptian Military Survey, 1989) is then applied to estimate the time varying baseline that yielded a 13.541 m root mean square height error between the SAR-estimated and the GCP-extracted heights. The estimated precise baseline length is 334.10 m. The unwrapped interferometric phase together with the precision baseline is then used to derive the topographic heights and true ground ranges based on the geometric relationships as described by Madsen *et al.* (1993) and Zebker *et al.* (1994). The interferometrically derived terrain heights (in slant range geometry) with 17.556 m range pixel spacing and 27.046 m azimuth pixel spacing shown in Fig. 4f are then orthonormalized in TCN coordinates, with the cross-track (C) coordinate following the Earth curvature (spherical Earth model). The rectification of the height data requires resampling in both azimuth and cross-track directions. Fig. 4g shows the shaded relief map of the 28.5 m resampled image with 100 m color cycle topographic fringes.

Geocoding (GEO) of the SAR range-Doppler coordinates to the orthonormal UTM coordinates involving the geometric transformation and the resampling together with interpolation of image data sets from SAR coordinate system to UTM coordinates. Backward and forward geocoding methodologies have been applied. The

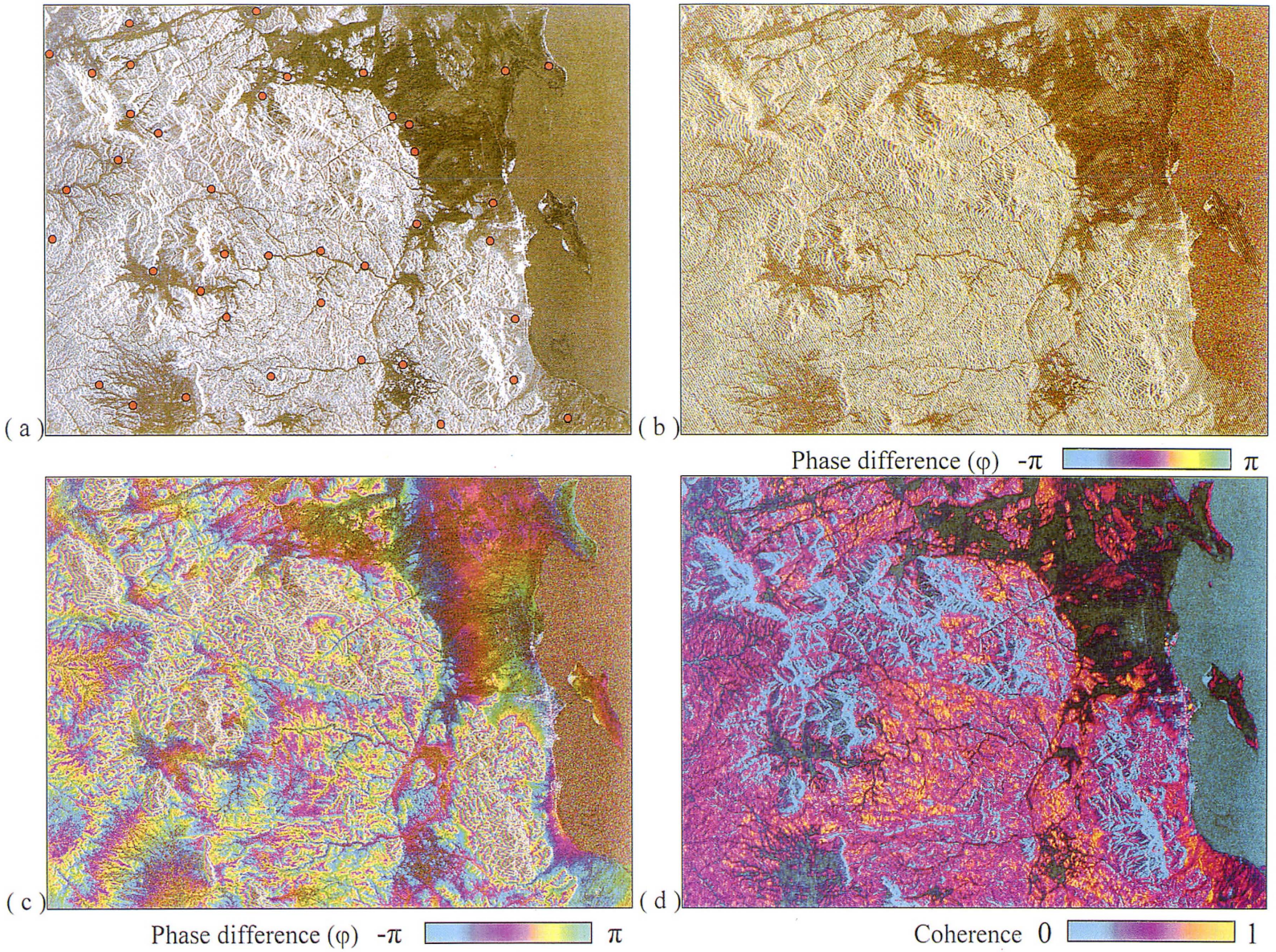

Fig. 4 JERS-1 InSAR products; (a) Master MLI image with 40 GCPs, (b) Interferogram, (c) Flat earth phase removed interferogram, (d) Coherence image, (e) Unwrapped phase image, (f) InSAR heights images in slant ranges, (g) Heights shaded-relief image, and (h) InSAR DEM UTM geocoded.

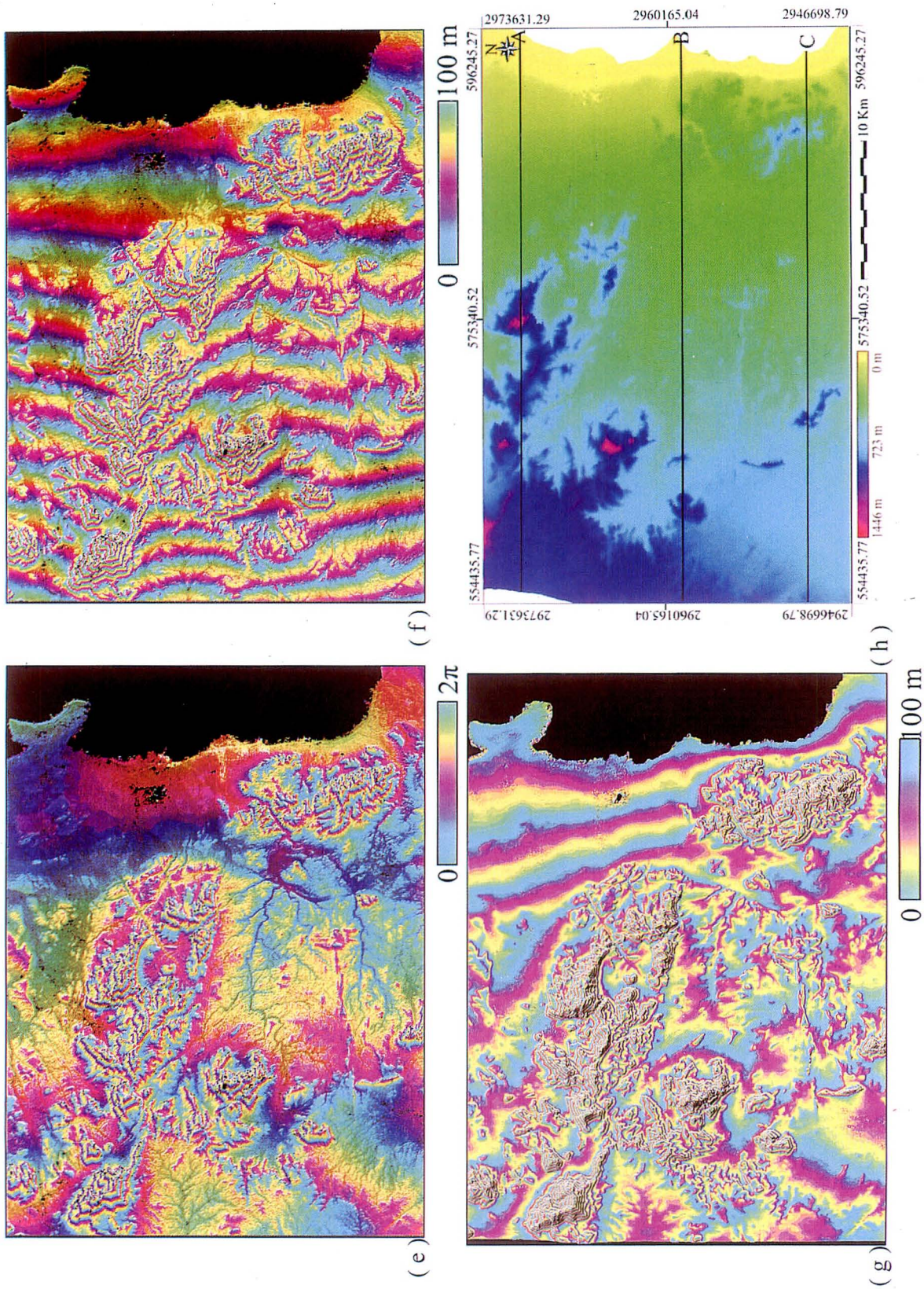

Fig. 4 Continued

generated DEM is then used to geocode all of the SAR products using the forward method, and then use the backward method later successively to terrain geocode all types of slant-range information (e.g. intensity, coherence, DEM, and other SAR products). The forward method is necessary when one has no reference elevation model, *i.e.* in the DEM generation application. The quality of the geocoding from the two methods is nearly identical (Small *et al.*, 1996).

For quality and accuracy improvements of the desired interferometric DEM, constraints such as coherence, phase unwrapping, and baseline were all balanced optimally and satisfied. The accuracy of the coherence estimates is improved through good cooregistration at sub-pixel accuracy and spectral band filtering of the two single-look complex images. Adaptive filtering to reduce the phase noise in low coherence areas facilitates phase unwrapping by adapting the filter window size with the relative coherence areas. Precise baseline is estimated applying a least square fit for a large number of ground control points well distributed through the scene avoiding local steep slope areas where phase unwrapping is problematic and height error estimates is relatively large. Quality check is of significant importance to move from one step to another and to optimally improve the final interferometric products. Based on these, the SAR processing parameters for DEM generation are optimized and satisfied.

2.3. InSAR post-processing

The resulted DEM, despite of its high resolution, coherence in some parts of the scene was very low (<0.075), due to effects like layover or shadowing (local steep slopes) resulted in phase unwrapping problems producing dislocations in the generated DEM. InSAR DEM was imported to GRASS GIS (GRASS Development Team) and the dislocation areas were interpolated using the regularized spline with tension approach to produce the final DEM (Fig. 4h).

3. InSAR DEM Validation

Validation of the InSAR derived DEM is carried out over such varying topography to explore the potential and limitations of the SAR technique before such data can be put into practical use. The height model validation is conducted through several techniques - visual and statistical. Visualisation of the accuracy surface is a quick method for error detection and can reveal pattern that is not reflected in the statistical measures. However, statistical methods through root mean square values together with histograms of the distribution of the height differences give more reliable results. The reference DEM is extracted from topographic maps at scale of 1:50,000 covering the study area, generated based on the work of Masoud *et al.* (2002).

Statistical analysis is conducted for the height differences between the reference model and the final InSAR DEM and indicated that the height estimates of the two DEMs agree remarkably well with mean absolute error of 17 ± 6 m for low relief areas with average slope of 4°, 8 ± 5m for moderate relief terrain with 13° average slope, and 21 ± 9m for highly rugged terrain areas with local steep slope of 32°. The height difference histogram is shown in Fig. 5a.

Visual interpretation included comparisons of terrain profiles across the two DEMs as well as a perspective 3-d view of the height difference map. Three profile sections are drawn across the height model and the reference DEM and proved quite good correspondence particularly where the rate of change in elevation is relatively low; with large height estimate deviations are confined to the steep slope areas (Fig. 5b). Further analysis was carried out to correlate the height differences with the coherence and slope variants (Table 1). Height differences are separated into classes to explore its relations with their contributing factors (coherence and slope). More than 60 % of the scene coverage have a coherence greater than 0.5 that assisted successful phase unwrapping. Fig. 5c shows the coherence histogram and Fig. 5d shows the slope histogram. This analysis concluded that height estimates are good enough in areas of moderate slope with suitable coherence, while steep slope low coherence areas as well as relatively high coherence flat areas are of large height deviations. A perspective 3-d view of the height difference classes is shown in Fig. 5e.

Large height deviations in steep slope hilly areas are due to effects like layover or shadowing, causing corrupted or no return signals from the terrain to the satellite antenna, while large height deviations in flat areas representing alluvial fans and stream channel floors may be due to surface changes resulted from topographic erosion and flash floods that affected the area under considerations before SAR data acquisition and after the topographic maps were generated. Such errors in height estimates can be reduced through processing of SAR data sets of different baselines. Further, InSAR DEM validation using up-to-date elevation models can give more reliable results.

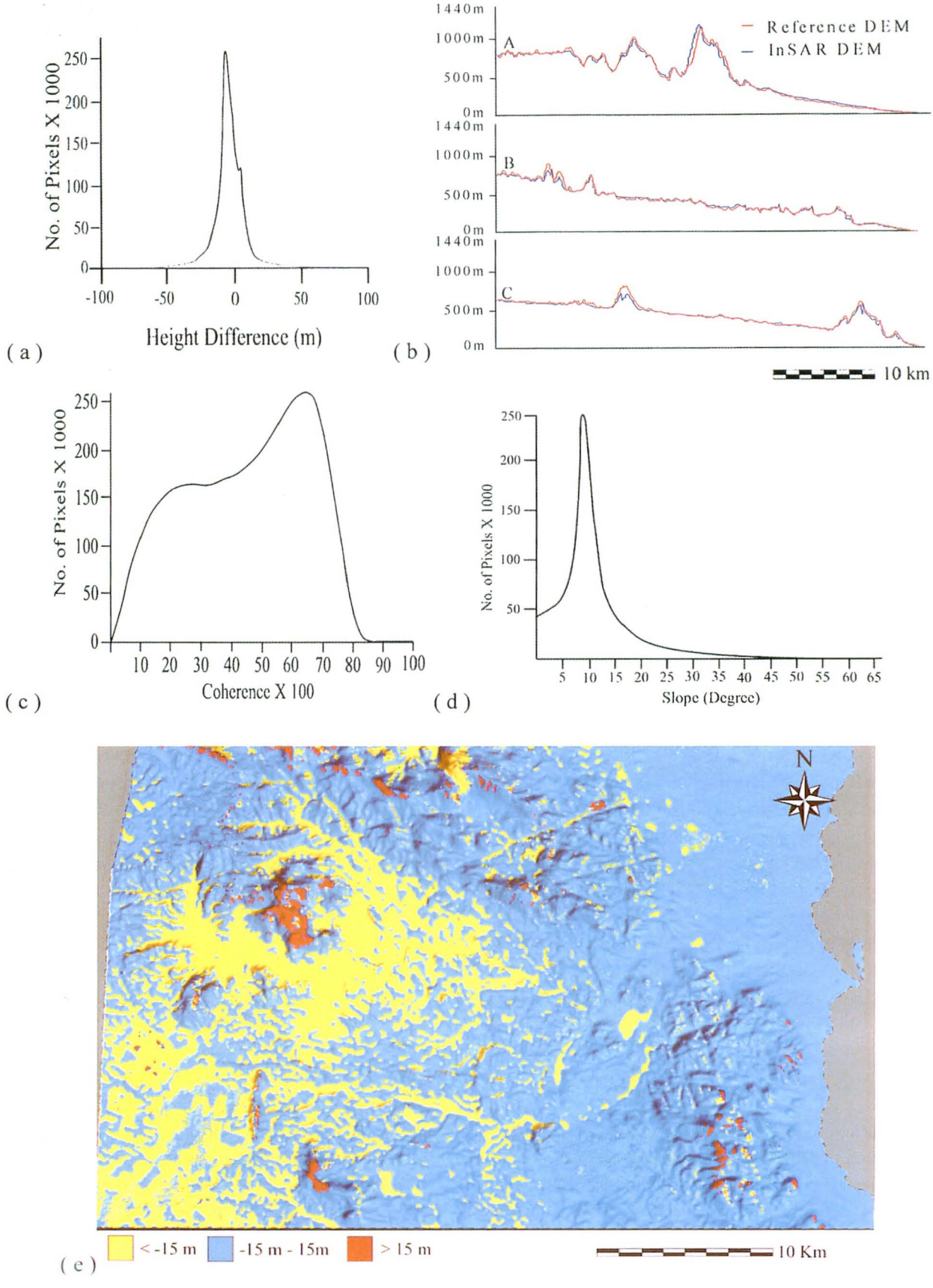

Fig. 5 InSAR DEM validation; (a) Height difference histogram, (b) Profile sections A, B, and C across the InSAR DEM and the reference DEM shown in Fig. 4 (h), (c) Coherence histogram, (d) Slope histogram, and (e) Height difference classes.

Table 1 Calculated statistics of the height difference classes against coherence and slope.

Height Diff. Classes	Percent Coverage %	Coherence Average	Slope (deg.) Average
< -15 m	21.50	0.61	4
-15 m – 15 m	77.27	0.53	13
> 15 m	1.23	0.20	32

4. Conclusions

The feasibility of large scale DEM generation with JERS-1 SAR interferometric technique has been validated over Safaga area where topography has significant variations. The SAR technique proved applicability for land surface modeling in such arid area due to the lack of impingement on the radar signal from vegetation and soil moisture, but areas of steep slope hindering the radar signal return to the satellite is another competing factor that needs to be solved.

Given the right conditions, good enough coherence, suitable baseline and precise baseline estimates, and successful phase unwrapping through justified data acquisition and optimal interferometric processing parameters, JERS-1 SAR interferometry can produce height models with respectable accuracy. Coherence must be maintained between acquisitions to allow reliable phase difference estimation. The baseline must be suitable to guarantee sufficient height sensitivity with a good spatial resolution and precise estimation of the baseline through sufficient number of ground control point distributed well over the terrain avoiding severely sloped areas facilitate accurate conversion from the relative unwrapped phase to the true ground heights. The slopes must not exceed limits dictated by the ambiguity resolvable during phase unwrapping. The weakness of JERS-1 InSAR height derivation lies in hilly rugged areas, where low coherences combine with topography to render height estimation problematic.

Methods that increase the scope of information considered promise improved reliability. For the improvement of the height estimates and the validation process, the SAR data acquisition and processing conditions (sensor parameters, baseline, temporal decorrelation, etc.) as well as landscape characteristics (slope, atmosphere, etc.) must be considered and optimally justified, and the reference DEM must be more accurate than the interferometric DEM itself representing the real terrain topography at the time of the SAR data acquisition. A comprehensive analysis through combination of different pairs with different baselines is advisable - in severely sloped areas, combination of such multi-baseline pairs is necessary to offer a more consistent ground resolution across the scene and could, in our opinion, lead to good qualitative and quantitative analysis for the InSAR DEM generation and validation in this test area.

Overall, the areal validation of 28.5 m InSAR DEM covering the test site provides confidence in the JERS-1 SAR technique. Automated DEM generation as well as the achievable quality and accuracy appraised the InSAR applicability in the area under concern, where such elevation data set is not available. The resulted DEM, despite of its acceptable errors, can be used as a database for many environmental modeling practices such as hydrological modeling for delineating drainage pathways, runoff contributing areas, and extraction of many hydrological parameters that could help in accessing the flash flood related hazards and mitigating such extreme weather events in the study area on a more realistic and sounded scientific basis.

References

Alaska SAR Facility (1999) The Alaska SAR Facility, http://www.asf.alaska.edu/

Egyptian Military Survey (1989) Topographic sheets of Safaga, Ras Abu Suma, Gabal Umm Inab and Gabal Wairah, scale 1:50000.

Goldstein, R. M., Zebker, H. A., and Werner, C. (1988) Satellite radar interferometry: two-dimensional phase unwrapping, *Radio Science*, **23**, 713-720.

Graham, L. C. (1974) Synthetic Interferometer Radar for Topographic Mapping. *Proceedings of IEEE*, **62**, 763-768.

GRASS GIS (GRASS Development Team), http://www3.baylor.edu/grass/

Li, F. K. and Goldstein, R. M., (1990) Studies of Multibaseline Spaceborne Interferometric Synthetic Aperture Radars, *IEEE Transactions on Geoscience and Remote Sensing*, **28**, 88-97.

Madsen, S. N., Zebker, H. A. and Martin, J. (1993) Topographic mapping using radar nterferometry: processing techniques, *IEEE Transsactions on Geoscience and Remote Sensing*, **31**, 246-255,

Masoud, Alaa, Masumoto Shinji, Raghavan Venkatesh, Kajiyama Atsushi, and Shiono Kiyoji (2002) Landscape Modeling and Analysis Based on Digital Elevation Models Generated from Topographic Maps: Algorithm and Application on Safaga Area, Red Sea Coast, Egypt, *Journal of Geosciences*, Osaka City Univ., **45**, 73-87.

Massonet, D., (1997) Satellite Radar Interferometry. Scientific American, Feb. 1997, 46-53.

Massonnet, D., (1995) Limitations to SAR Interferometry due to Instrument, Climate or Target Geometry Instabilities. *EARSeL Advances in Remote Sensing, Topography from Space*, **4**, October 1995, 19-25.

Rosen P. A., Werner, C. L., and Hiramatsu, A., (1994) Two-dimensional Phase Unwrapping of SAR Interferograms by Charge Connection Through Neutral Trees, *Proceedings of IGARSS'94, JPL, Pasadena 1994.*

Small D., Pasquali, P., Füglistaler, S., (1996) A Comparison of Phase to Height Conversion Methods for SAR Interferometry, *Proceedings of IEEE-IGARSS'96*, Lincoln, Nebraska, USA, 342-344.

Werner C., Wegmüller, U., Strozzi, T., and Wiesmann, A. (2000) Gamma SAR and Interferometric Processing Software, *Proceedings of ERS-ENVISAT Symposium, Gothenburg, Sweden*, 16-20 Oct. 2000.

Zebker, H. A. and Goldstein, R. M., (1986) Topographic Mapping from Interferometric SAR Observations. *Journal of Geophysical Research*, **91**, 4993-4999.

Zebker, H. A. and Villasenor, J. (1992) Decorrelation in Interferometric Radar Echoes. *IEEE Transsactions on Geoscience and Remote Sensing*, **30**, 950-959.

Zebker, H. A., Rosen, P., Goldstein, R. M., Gabriel, A., and Werner, C. L., (1994) On the derivation of coseismic displacement fields using differential radar interferometry: the Landers earthquake, *Journal of Geophysical Research*, **99**, 19617-19634.

Manuscript received August 22, 2002.
Revised manuscript accepted November, 2002.